

## Antiferromagnetic order in the $\delta$ phase of solid oxygen

Federico A. Gorelli,<sup>1,3,\*</sup> Lorenzo Ulivi,<sup>2,†</sup> Mario Santoro,<sup>1,3,‡</sup> and Roberto Bini<sup>3,4,§</sup>

<sup>1</sup>*Dipartimento di Fisica dell'Università di Firenze and INFM, Largo Enrico Fermi 2, I-50125 Firenze, Italy*

<sup>2</sup>*Istituto di Elettronica Quantistica, Consiglio Nazionale delle Ricerche, and INFM, Via Panciatichi 56/30, I-50127 Firenze, Italy*

<sup>3</sup>*LENS, European Laboratory for Non-linear Spectroscopy, Largo Enrico Fermi 2, I-50125 Firenze, Italy*

<sup>4</sup>*Dipartimento di Chimica dell'Università di Firenze, Via Gino Capponi 9, I-50121 Firenze, Italy*

(Received 12 May 2000)

Infrared spectroscopy has been applied to the study of solid oxygen in the pressure-temperature region enclosed among the  $\alpha$ ,  $\beta$ , and  $\epsilon$  phases which is now unambiguously assigned to the  $\delta$  phase. The narrow peak, detected in the fundamental mode region, is assigned to a vibron component allowed because of the long-range antiferromagnetic order of the molecular spins which, as in the  $\alpha$  phase, produces a doubling of the primitive cell. The integrated infrared absorption evolution with temperature confirms this model. The molecular vibrational coupling is quantitatively interpreted as due to the Heisenberg interaction via the exchange integral  $J$ .

Among simple molecular crystals solid oxygen constitutes an interesting localized-spin system where magnetism comes from a direct overlap of molecular orbitals.<sup>1</sup> The magnetic interaction is fundamental to stabilize the peculiar molecular arrangement in the crystal.<sup>2</sup> The difficulty to obtain high quality single crystals at low temperature and high pressure makes a direct optical spectroscopic detection of the magnetic signatures due to spin waves (magnons) extremely hard, but the interaction between magnetic and structural properties can also induce the activity of new vibrational modes whose behavior can be studied as a function of temperature or external applied magnetic fields. These effects have been observed in the lowest-temperature phase of oxygen at zero pressure:<sup>3</sup> the monoclinic ( $C2/m$ )  $\alpha$ -O<sub>2</sub>.<sup>4</sup> The  $\alpha$ -O<sub>2</sub> crystal is the only elemental solid that is both insulating and antiferromagnetic, and then the only known antiferromagnetic molecular crystal.<sup>5</sup> In this phase all spins are aligned along the monoclinic  $b$  axis with an opposite orientation in nearest-neighbor molecules. This arrangement determines a primitive magnetic cell ( $Cp2/m$ ) containing two inequivalent molecules.<sup>6</sup> Above 24 K, at atmospheric pressure, the  $\alpha$  phase transforms into the rhombohedral ( $R\bar{3}m$ )  $\beta$  phase where only a short-range antiferromagnetic order is present.<sup>7</sup> The  $\alpha$ - $\beta$  phase transition takes place with negligible volume change and heat of transformation, and the relative slight structural distortions are interpreted as essentially due to magnetic effects.<sup>7,8</sup> At low temperature the region extending between the  $\alpha$  and the  $\epsilon$  phases is not yet definitely assigned. Two phases,  $\alpha'$  and  $\delta$  in order of increasing pressure, were suggested on the basis of Raman studies.<sup>9</sup> The existence of the  $\alpha'$  phase is not confirmed by other Raman<sup>10</sup> and recent infrared experiments.<sup>11</sup> At room temperature and 9.6 GPa the structure of the  $\delta$  phase has been determined to be orthorhombic ( $Fmmm$ ,  $D_{2h}^{23}$ ) with one molecule per primitive cell. Molecules are aligned parallel and form molecular planes as in the  $\alpha$  and  $\beta$  phases.<sup>12</sup> Lattice dynamics<sup>13</sup> and *ab initio*<sup>14</sup> simulations obtain the correct  $Fmmm$  structure of the  $\delta$  phase with one molecule in the crystallographic primitive cell and with an antiferromag-

netic order of the oxygen spins. Experimental evidences confirming this latter expectation are still missing.

In a previous report we investigated the infrared spectrum at low temperature from 2 GPa up to the  $\delta$ - $\epsilon$  transition.<sup>11</sup> We detected an absorption line in the vibron fundamental mode region not expected according to the  $Fmmm$  crystal symmetry. Those results prompted us to scan finely the phase diagram along isobaric cooling and heating cycles at different pressures, and along isothermal compression paths, by using Fourier transform infrared (FTIR) spectroscopy. Our data do not confirm the phase transitions reported by Jodl *et al.*<sup>9</sup> and by Yen and Nicol,<sup>15</sup> and we assign the whole region extending among the  $\alpha$ ,  $\beta$ , and  $\epsilon$  phases to the  $\delta$  phase. In the following we will show clear evidence of the expected antiferromagnetic character of the  $\delta$  phase. This effect is, in our opinion, strongly correlated to the formation of the O<sub>4</sub> molecule whose existence, in the high-pressure  $\epsilon$  phase, we have recently shown.<sup>16</sup>

High-purity oxygen was filled into a membrane diamond-anvil cell (MDAC) by means of the cryogenic loading technique. The details of our optical setup for Fourier transform infrared measurements with the MDAC have been carefully described elsewhere.<sup>16,17</sup> Oxygen was slowly cooled (0.2–0.3 K/h) through the melting line at 6 GPa into the  $\beta$  phase. Four isobaric cooling and heating cycles have been performed at 7.0, 5.8, 5.0, and 4.5 GPa from 15 to 200 K. In spite of the polycrystalline nature of our samples, a good crystal quality is attested by the narrow absorption vibron line observed in the experiments performed following the sample preparation described above.

In Fig. 1 we show the fundamental vibron peak of oxygen, measured along the 7.0 GPa isobar increasing temperature from 13.8 K to 205.6 K, i.e., very close to the  $\delta$ - $\beta$  phase transition. The intensity of this spectral line decreases continuously rising temperature and vanishes as the  $\beta$  phase is reached. The same behavior was observed in all the other isobaric measurements. From the spectral fit we have obtained the linewidth, which always exceeds the instrumental resolution ( $1 \text{ cm}^{-1}$ ) ranging between 1.5 and  $2.5 \text{ cm}^{-1}$ , the frequency peak values, and the integrated intensity. The

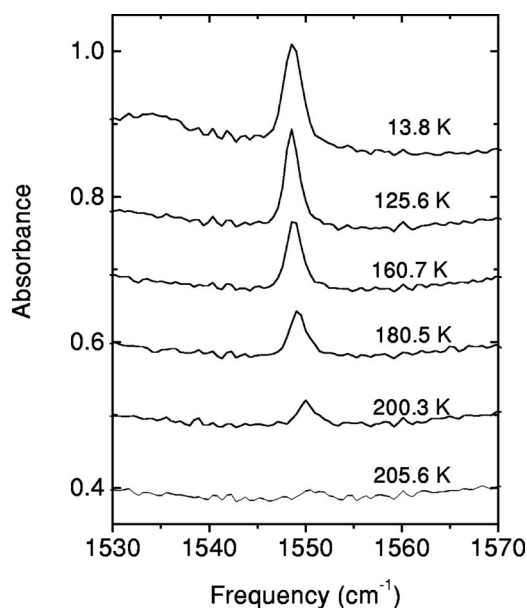


FIG. 1. Infrared spectra, vertically shifted, recorded along the 7 GPa isobar increasing temperature.

analysis of the full set of parameters as a function of pressure or temperature does not show discontinuities, suggesting that the whole investigated region belongs to the  $\delta$  phase. In Fig. 2 we report the integrated absorbance as a function of temperature. Specifically, in the insert we show the raw data relative to the 7.0 GPa experiment. Full and open dots concern, respectively, the cooling and the warming run revealing an evident hysteresis which affects the entire temperature cycle. A similar effect has been observed at every investigated pressure. We have also monitored the kinetics during a time interval of about 12–15 h at several fixed temperatures observing a very slow increase (or decrease) of the peak intensity with time along the cooling (or warming) path. This fact indicates that the measured intensities correspond to

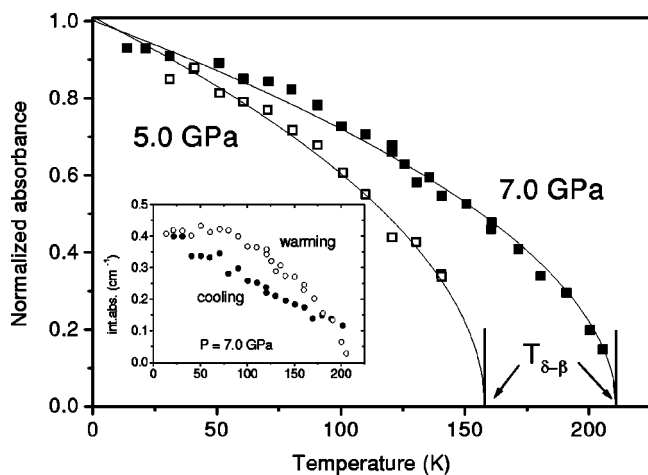


FIG. 2. Evolution with temperature of the normalized absorbance along different isobars. The data (squares) have been obtained by averaging the values recorded during the cooling and warming cycles. Full lines fit the data according to the law  $I = (1 - T/T_N)^{0.5}$ . The full segments indicate the  $T_{\delta-\beta}$  values at 5 GPa (158 K) and 7 GPa (211 K). The original data obtained in the 7 GPa run are shown in the inset.

metastable states. Therefore, in order to obtain the equilibrium values, we calculated the average absorbance between the cooling and the warming cycles. In Fig. 2 the values obtained according to this procedure are reported as squares for two different isobars, normalized with respect to the absorbance extrapolated to zero temperature.

In the unit cell of  $\delta$  oxygen the molecules lie on sites having  $D_{2h}$  symmetry, then only one Raman band in the fundamental mode region is expected.<sup>11</sup> The sharp infrared band observed in the  $\delta$  phase, which cannot be ascribed to crystal stress or defects, is interpreted in terms of antiferromagnetic ordering of the oxygen molecular spins. In this case the magnetic primitive cell will contain the two molecules on the vertex and on the basis center of the conventional  $Fmmm$  cell, with antiparallel spins, as it happens for the  $\alpha$  phase.<sup>6</sup> The Raman and the infrared modes are interpreted as the in- and out-of-phase stretching motions of the pair of molecules. The charge transfer mechanism strongly contributes to the induced dipole moment of the pair allowing the detection of the infrared vibron peak at high pressure. The missing observation of the analogous infrared mode in the  $\alpha$  phase is only due to a smaller transition dipole moment related to the larger separation between the two molecules.

A direct probe of the antiferromagnetic origin of the infrared vibron peak is represented by the analysis of the temperature dependence of the absorption intensity shown in Fig. 2. The temperature increase reduces the spin long-range order and then the intensity of the infrared band. The temperature behavior of the normalized absorbance  $I$  has been fitted with the power law  $I = (1 - T/T_N)^\beta$  obtaining, within the errors,  $\beta = 0.5$  for all the pressures. Here,  $T_N$  is the temperature of the  $\delta$ - $\beta$  transition as given in the literature.<sup>18</sup> The proportionality between the absorbance of the infrared vibron line and the square of the order parameter  $\sigma$  was demonstrated to hold in order-disorder phase transitions related to two quite different solid systems like deuterium<sup>19</sup> and nitrogen.<sup>20</sup> Since also in this case an order-disorder phenomenon (spin alignment) is the basis of the infrared absorption, we assume the same relation resulting in the law  $\sigma = (1 - T/T_N)^{0.25}$ . The exponent value is lower than that ( $\approx 0.33$ ) obtained for most real and model three-dimensional (3D) systems, but it is higher than the value expected by the 2D Ising model (1/8).<sup>21</sup> As a matter of fact, the lack of data very close to the critical temperature does not allow the identification of the exponent with the critical parameter. An additional complication is due to the presence of the structural transition to the  $\beta$  phase which, as for the  $\alpha$ - $\beta$  transition,<sup>22</sup> precludes a definitive interpretation of  $T_N$  as the Néel temperature. An accurate investigation of the infrared intensity close to  $T_N$  could provide a better insight, beyond the scope of the present report, on the relative weights of the coupling between molecules within the  $ab$  layers with respect to that connecting molecules in different planes of the crystal.

In our previous report we used the Davydov splitting of the fundamental mode to determine the vibrational coupling parameter  $G$ .<sup>11</sup> Surprising was its positive sign and its strong dependence on the intermolecular distance. We will show that the magnetic interaction induces this vibrational coupling. The Heisenberg antiferromagnetic Hamiltonian is

$$H_{12} = -J_{12} \hat{S}_1 \cdot \hat{S}_2, \quad (1)$$

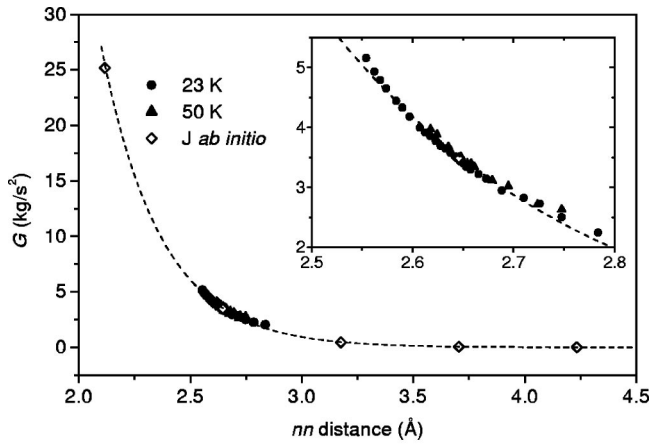


FIG. 3. Full symbols are the experimental  $G$  values: dots from Ref. 11; triangles from present work. Empty symbols are *ab initio*  $J$  values from Ref. 23, scaled on the experimental data and fitted with an exponential (dashed line).

where  $\hat{S}_1$  and  $\hat{S}_2$  are the molecular spin operators and  $J_{12}$ , which is negative, is the exchange integral. Usually Eq. (1) is written for two rigid and fixed molecules, while the spins are the only variables. More generally, the quantity  $J_{12}$  depends on the molecular coordinates. We are interested in the dependence of  $J$  on the intermolecular distance  $R$  and on the internuclear distance  $r_1$  and  $r_2$ . For nearest neighbor (nn) in the  $\delta$  phase  $J_{12}(R, \vec{r}_1, \vec{r}_2)$  can be expanded up to the second order in terms of  $x_i = r_i - r_e$  ( $i = 1, 2$ ) leading to

$$H_{12} = -\hat{S}_1 \cdot \hat{S}_2 \left\{ J_{12}^0(R, r_e, r_e) + \frac{1}{2} \frac{\partial^2 J_{12}}{\partial x_1^2} \Big|_{x_1=x_2=0} (x_1^2 + x_2^2) + \frac{\partial^2 J_{12}}{\partial x_1 \partial x_2} \Big|_{x_1=x_2=0} x_1 x_2 \right\}, \quad (2)$$

where  $r_e$  is the equilibrium internuclear distance. The second and the third term in parenthesis appear then as the magnetic contributions to the single molecule and pair vibrational energy, respectively. Neglecting other coupling mechanisms,  $G$  has to be interpreted as the averaged third term of Eq. (2), that is

$$G = -\langle \hat{S}_1 \cdot \hat{S}_2 \rangle_T \frac{\partial^2 J_{12}}{\partial x_1 \partial x_2} \Big|_{x_1=x_2=0} \quad (3)$$

resulting then proportional to the  $nn$  spin-correlation function  $\langle \hat{S}_1 \cdot \hat{S}_2 \rangle_T$ . The experimental density dependence of  $G$ , as obtained by the difference of the infrared and Raman data at 23 and 50 K (Ref. 11) and on the basis of the computed EOS for solid oxygen in this region,<sup>13</sup> can be compared to that calculated for the exchange integral  $J_{12}$ .<sup>23</sup> Here we assume that the small modulation of  $J_{12}$ , due to the vibrational motion, could be factored out from the dependence on the  $nn$  distance  $R$ . Furthermore, the density dependence of the  $nn$  spin-correlation function has been neglected since the temperature is low and far from that of the  $\delta$ - $\beta$  phase transition. In Fig. 3 we show the comparison between the experimental  $G$  and the *ab initio* values of  $J_{12}(R)$  scaled with a factor and

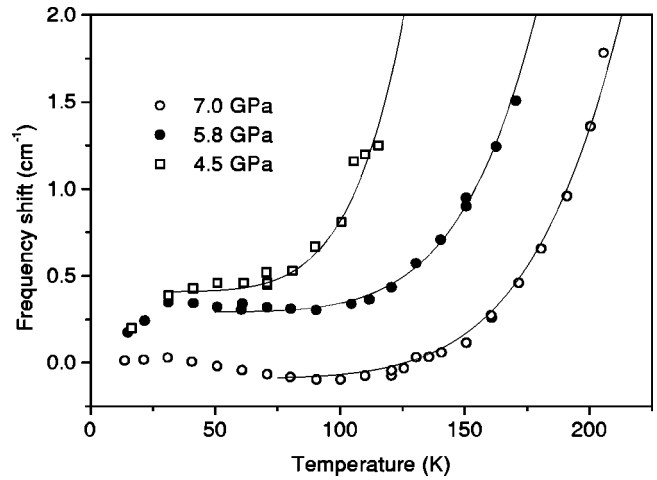


FIG. 4. Frequency evolution on the temperature of the infrared peak along different isobaric paths. Full lines result from a fit analysis according to a power law proportional to  $T^6$ .

fitted (dashed line) with an exponential in the whole range of the calculation. The evolution of  $G$  is very well described by this curve in the overlapping region (2.5–2.8 Å) confirming its magnetic origin.

On the basis of Eq. (2) we can model also the magnetic contribution to the temperature behavior of the IR vibrational frequency obtaining

$$\nu_{IR}(cm^{-1}) = \frac{1}{2\pi c} \left( \frac{k - \langle \hat{S}_1 \cdot \hat{S}_2 \rangle_T (a - 4b)}{\mu} \right)^{1/2}; \quad (4)$$

$$a = \frac{1}{2} \frac{\partial^2 J_{12}}{\partial x_1^2} \Big|_{x_1=x_2=0}; \quad b = \frac{\partial^2 J_{12}}{\partial x_1 \partial x_2} \Big|_{x_1=x_2=0},$$

where  $k$  is the elastic constant perturbed by all nonmagnetic crystal field contributions. The evolution of the infrared mode frequency with temperature is illustrated for different isobars in Fig. 4. To compare the different results we report the shift with respect to the extrapolated frequencies at  $T = 0$  K. At low temperature the curves show an almost flat behavior with a reproducible steep increase about 80–100 K below the  $\delta$ - $\beta$  phase transition. We used a  $T^6$  power law to reproduce the strong temperature dependence. This behavior cannot be explained on the basis of anharmonic interaction processes, so we ascribe it to the spin-correlation function whose absolute value decreases for increasing temperature. Furthermore, since this term is negative for an antiferromagnet, in order to reproduce the experimental frequency increase, it results that  $a < 4b$ . We want to remark that from this single spectroscopic experiment on the vibron mode a precise, though indirect, information is obtained both on the short-range spin-correlation function (by the pressure and temperature evolution of the frequency) and on the long-range order of a magnetic system (by the temperature evolution of the intensity).

According to the present results we are able to draw the evolution of the intermolecular interactions in solid oxygen at low temperature as the pressure is increased. Electronic exchange is responsible of the magnetic interaction among

oxygen molecules leading to an antiferromagnetic ordering in the  $\alpha$  phase. In the  $\delta$  phase the observation of the infrared vibron peak is not consistent with the crystal structure according to which only one Raman mode is expected. We interpret the appearance of the vibron peak as due to the antiferromagnetic order which causes the doubling of the cell allowing the in-phase (Raman active) and out-of-phase (infrared active) optical modes of the two molecules forming the magnetic primitive cell. The temperature evolution at constant pressure of the infrared vibron absorbance is consistent with the antiferromagnetic order of the  $\delta$  phase. Also the vibrational coupling is interpreted in term of  $m$  spin

correlation and results proportional to the exchange integral  $J$ . This explains the strong density dependence of  $G$  with a very good agreement with theoretical *ab initio* results for  $J$ . The antiferromagnetic coupling between nearest-neighbor  $O_2$  molecules is therefore responsible for the increasing molecular interaction in the  $\delta$  phase. The  $\delta$ - $\epsilon$  phase transition acts as a kind of reversible chemical reaction whose product are  $O_4$  units in a singlet state.<sup>16</sup>

Discussions with M. G. Pini and A. Rettori are gratefully acknowledged. This work has been supported by the European Union under Contract No. ERB FMGE CT 950017.

\*Electronic addresses: gorelli@lens.unifi.it

†Electronic address: ulivi@ieq.fi.cnr.it

‡Electronic address: santoro@lens.unifi.it

§Electronic address: bini@chim.unifi.it

<sup>1</sup>G. C. DeFotis, Phys. Rev. B **23**, 4714 (1981).

<sup>2</sup>M. Nicol and K. Syassen, Phys. Rev. B **28**, 1201 (1983).

<sup>3</sup>K.D. Bier and H.J. Jodl, J. Chem. Phys. **81**, 1192 (1984).

<sup>4</sup>C.S. Barrett, L. Meyer, and J. Wassermann, J. Chem. Phys. **47**, 592 (1967).

<sup>5</sup>R.J. Meier and R.B. Helmholtz, Phys. Rev. B **29**, 1387 (1984).

<sup>6</sup>A.P.J. Jansen, J. Phys. C **21**, 4221 (1988).

<sup>7</sup>R. LeSar and R.D. Ethers, Phys. Rev. B **37**, 5364 (1987).

<sup>8</sup>A.P.J. Jansen and A. Van der Avoird, J. Chem. Phys. **86**, 3583 (1987).

<sup>9</sup>H.J. Jodl, F. Bolduan, and H.D. Hocheimer, Phys. Rev. B **31**, 7376 (1985).

<sup>10</sup>R.J. Meier, M.P. Van Albada, and A. Lagendijk, Phys. Rev. Lett. **52**, 1045 (1984).

<sup>11</sup>F.A. Gorelli, L. Ulivi, M. Santoro, and R. Bini, Phys. Rev. B **60**, 6179 (1999).

<sup>12</sup>D. Schiferl, D.T. Cromer, L. Schwalbe, and R.L. Mills, Acta

Crystallogr., Sect. B: Struct. Sci. **B39**, 153 (1983).

<sup>13</sup>R.D. Ethers, K. Kobashi, and J. Belak, Phys. Rev. B **32**, 4097 (1985).

<sup>14</sup>S. Serra, G. Chiarotti, S. Scandolo, and E. Tosatti, Phys. Rev. Lett. **80**, 5160 (1998).

<sup>15</sup>J. Yen and M. Nicol, J. Phys. Chem. **87**, 4616 (1983).

<sup>16</sup>F.A. Gorelli, L. Ulivi, M. Santoro, and R. Bini, Phys. Rev. Lett. **83**, 4093 (1999).

<sup>17</sup>R. Bini, R. Ballerini, G. Pratesi, and H.J. Jodl, Rev. Sci. Instrum. **68**, 3154 (1997).

<sup>18</sup>B. Olinger, R.L. Mills, and R.B. Roof, J. Chem. Phys. **81**, 5068 (1984).

<sup>19</sup>L. Cui, N.H. Chen, and I.F. Silvera, Phys. Rev. B **51**, 14 987 (1995).

<sup>20</sup>R. Bini, M. Jordan, L. Ulivi, and H.J. Jodl, J. Chem. Phys. **108**, 6849 (1998).

<sup>21</sup>N.W. Ashcroft and N.D. Mermin, *Solid State Physics* (Holt-Saunders, Tokyo, 1981).

<sup>22</sup>P.W. Stephens and C.F. Majkrzak, Phys. Rev. B **33**, 1 (1986).

<sup>23</sup>P.E.S. Wormer and A. van der Avoird, J. Chem. Phys. **81**, 1929 (1984).